MILLIMETER ARRAY
MEMO NO. 115

POLARIZATION PROPERTIES OF AN OPEN CASSEGRAIN ANTENNA

Peter J. Napier
NRAO, Socorro.
May 4, 1994.

ABSTRACT

The offset geometry of the Open Cassegrain antenna design proposed for the MMA will cause circulary polarized beams to be separated by 0.14 beamwidths, compared with a separation of 0.06 beamwidths for the VLA. If uncorrected this circular polarization beam squint will seriously limit the ability of the MMA to measure circular polarization. Two methods are proposed to correct this polarization degradation. Both of these solutions require the addition of reflectors in the optical path and need further study to be sure that there are no undesired diffraction effects in the longest MMA wavelength bands.

1. INTRODUCTION

A Millimeter Array (MMA) antenna design using an offset Cassegrain geometry offers a number of attractive advantages including light weight (and therefore low cost), reduced reflector gravitational deformations and reduced blockage (Cheng, 1994). A significant disadvantage of the design is a degradation in the polarization performance of the antenna resulting from the loss of symmetry in the offset geometry. In this report we investigate this loss of polarization performance.

We will use the term "offset reflector" to mean a reflector which is part of a symmetric conic surface of revolution (paraboloid, ellipsoid, hyperboloid) but which, because its center does not coincide with the axis of symmetry of the parent surface, is itself asymmetric. The polarization problems of a prime-focus-fed offset parabola are well known (Chu and Turrin, 1973) to include high cross polarized sidelobes for linearly polarized feeds and non-coincident beams (beam squint) for circularly polarized feeds.

Rudge et al (pg 188, 1982) classifies offset Cassegrain antennas into the three types shown in Figure 1. In the double offset system the secondary focus is located on the axis of symmetry of the parent parabola (of which the offset primary reflector is a piece). This geometry has similar polarization problems to the prime-focus offset system, somewhat reduced in magnitude because of the longer effective focal length. In the optimized double offset geometry (Figure 1b) the axis of the subreflector is rotated through a small angle, so that the secondary focus is located a small distance off of the axis of the parent parabola, and the polarization problems are cured provided the rotation angle is correctly chosen as explained in Section 2 below. The geometry of the GBT is an example of an

optimized double offset geometry (except that the GBT is Gregorian rather than Cassegrainian) and the GBT will have good polarization performance at its secondary focus. The geometry proposed for the MMA by Cheng (1994) is an example of an Open Cassegrain (Figure 1c). Here the subreflector axis is rotated by a large angle so that the secondary focus is far away from the parent parabola axis in the middle of the offset primary reflector. The polarization correction of the optimized design is no longer possible and the Open Cassegrain has poor polarization performance (pg 234, Rudge et al 1988, Chu and Turrin, 1973). In Section 2 we provide the formulas needed to calculate the magnitude of this degradation and in Section 3 we apply the formulas to the MMA and other Open Cassegrain designs. In Section 4 we consider the astronomical consequences of the degradation and in Section 5 we discuss possible solutions if the degradation is unacceptable.

2. POLARIZATION PROPERTIES OF OFFSET DUAL REFLECTOR ANTENNAS

Consider first a single reflector antenna (Figure 2). If a parabola , with focal length F, is fed by a circularly polarized feed whose phase center is located on the prime focus of the parabola and whose axis is tilted by an angle θ_0 with respect to the parabola axis, then the beam from the parabola is squinted away from the parabola axis by an angle θ_s given by (Duan and Rahmat-Samii, 1990):

$$\theta_s = \mp \sin^{-1}\left(\frac{\sin\theta_0}{2Fk}\right) \qquad (1)$$

where $k=2\pi/\lambda$ and λ is the wavelength. The direction of the beam squint is orthogonal to the plane containing the axis of the parabola and the axis of the feed. The $\mp$ sign means that the right circularly polarized (RCP) beam is squinted to the left (looking from the parabola vertex out along the parabola axis) and the LCP beam is squinted to the right. The total separation between the two beams is then $2\theta_s$ and is independent of frequency when expressed as a fraction of the beamwidth. Note that (1) applies to a symmetric or an offset parabola and indicates that, provided the feed has good polarization performance such as is provided by a corrugated horn, there will be no circularly polarized beam squint if the feed axis is parallel to the parabola axis.

If the feed in Figure 2 is linearly, instead of circularly, polarized the linearly polarized beams are not squinted but a pair of cross polarized sidelobes are present with peaks located at about the -5dB points of the main beam. These cross polarized sidelobes lie in the plane orthogonal to the plane containing the parabola axis and the feed axis. We have used the approach of

Thompson (1973), in which the linear cross polarization is obtained from the phase shift of the circular polarization, to estimate the size of these cross polarized sidelobes and the results are shown in Figure 3. Note that the curves in Figure 3 are in good agreement with the results in Chu and Turrin (1973).

We will now consider dual reflector offset antennas. We will use the approach of Rusch et al (1990) and Duan and Rahmat-Samii (1991) in which a prime focus fed offset parabola is defined which is equivalent in performance to the dual reflector antenna. The equivalent parabola is equivalent in the sense that, if it is fed from its prime focus by the same feed as is used for the dual reflector antenna, it will have the same copolarized and crosspolarized radiation patterns as the dual reflector antenna. Once the equivalent parabola is found expression (1) and the curves of Figure 3 can be used to quantify the polarization performance of the dual reflector system. The geometry of the dual reflector system is shown in Figure 4. The axis of the subreflector is rotated by an angle β with respect to the parabola axis and the axis of the feed is rotated by an angle θ_β with respect to the subreflector axis. The focal length, F_{eq}, of the equivalent parabola is given by (Rusch et al, 1990):

$$F_{eq} = F \times \frac{|e^2-1|}{(e^2+1) - 2e\cos(\beta)} \qquad (2)$$

where e is the ellipticity of the subreflector. Note that in the case of a symmetrical dual reflector system $\beta=0$ and (2) reduces to the well known result that the effective focal length is the product of the primary focal length and the magnification, where the magnification is $(e+1)/(e-1)$. The angle, α, between the subreflector axis and the axis of the equivalent paraboloid is given by:

$$\tan\left(\frac{\alpha}{2}\right) = \frac{e+1}{e-1}\tan\left(\frac{\beta}{2}\right) \qquad (3)$$

Note that there is a quadrant ambiguity for α in (3). This ambiguity can be resolved using the fact (Dragone, 1978) that the axis of the equivalent parabola passes through the secondary focus and the point of intersection of the real parabola axis with the subreflector surface. Note that to find this point of intersection it may be necessary to draw the entire ellipse in the case of a Gregorian secondary or to draw the second branch of the hyperbola in the case of a Cassegrain secondary. The angle that the feed axis is rotated with respect to the equivalent

parabola axis is $\theta_\beta-\alpha$ so we can use (1) to determine the beam squint, θ_s, of the dual reflector as :

$$\theta_s = \pm \sin^{-1}\left(\frac{\sin(\theta_\beta-\alpha)}{2F_{eq}k} \right) \qquad (4)$$

Equation (4) indicates that if it can be arranged that $\theta_\beta-\alpha = 0$, that is the feed is pointed along the axis of the equivalent parabola, there is no beam squint. This is the case for the optimized double offset geometry mentioned in Section 1. (2) and (4) show that as the subreflector axis offset angle, β, increases F_{eq} decreases and the beam squint increases. With the Open Cassegrain geometry β is so large that it is not possible to have the feed both aligned with the equivalent parabola axis and pointed at the center of the subreflector at the same time so the beam squint cannot be avoided.

3. POLARIZATION PROPERTIES OF OPEN CASSEGRAIN ANTENNAS

Before applying the formulas in Section 2 to the MMA design we will check them using two Open Cassegrain antennas whose polarization properties are known.

The VLA antenna can be thought of as a special case of an Open Cassegrain geometry in which the subreflector axis is rotated to locate the secondary focus off the axis of the primary but the primary reflector happens to be symmetric. The shaped reflectors of the VLA were derived as small perturbations on the parent classical Cassegrain geometry shown in Figure 5. Since polarization degradation of the type considered in this report is almost independent of aperture illumination taper it is expected that the beam squint of the classical Cassegrain and the shaped Cassegrain will be almost the same. The parameters for the VLA geometry are F = 9.0 m, e = 1.26, $\beta = 7.55^\circ$, $\theta_\beta = 1^\circ$. Expressions (2) and (3) then give F_{eq}= 59.1 m and $\alpha = 59.8^\circ$. For λ = 6cm (4) then gives θ_s = 14.3 arcsec which corresponds to .029 λ/D, where D is the diameter of the primary aperture, or .027 θ_{FWHM}, where θ_{FWHM} is the half power beamwidth. This is in good agreement with measurements of the VLA antennas which show that the total beam separation is about .06 beamwidths (Vourlidas and Bastian, 1993 - note that in this reference there is occasionally confusion between the squint of the individual LCP and RCP beams and the total offset between the two beams).

An Open Cassegrain antenna which is very similar to the proposed MMA design, and in fact is also a slant axis design, is described by Cook et al (1965). The geometry of this antenna, scaled to the MMA aperture diameter of 8 m, is shown in Figure 6 and has the following parameters. F = 6.06 m, e = 1.63, β =

47.5°, θ_β = 0. Expressions (2) and (3) then give F_{eq}= 6.9 m and α = 122.9°. For λ = 1 cm (4) then gives θ_s = 20.9 arcsec which corresponds to .081 λ/D. The curves of Figure 3 then predict linearly polarized sidelobes of -22.5 dB which agrees well with the -23 dB value computed by Cook et al (1965).

The geometry proposed by Cheng (1994) for the MMA is shown in Figure 7 and has the following parameters. F = 5.0 m, e = 1.14, β = 45.0°, θ_β = 0. Expressions (2) and (3) then give F_{eq}= 2.18 m and α = 17.5°. For λ = 1 cm (4) then gives θ_s = 22.6 arcsec which corresponds to .088 λ/D. For a -10 dB aperture illumination edge taper the half power beamwidth, θ_{FWHM}= 1.24 λ/D so the total offset between the two circularly polarized beams expressed as a fraction of a beamwidth is $2\theta_s/\theta_{FWHM}$ = .14 beamwidths. The curves of Figure 3 then predict linearly polarized sidelobes of -22.0 dB with respect to the peak of the copolarized beam or -15.5 dB with respect to the gain of the main beam at the same angle as the peak of the cross polarization. One additional problem with this geometry should be noted. The subreflector does not subtend equal angles around the feed axis which would result in asymmetric illumination in the aperture. This problem can be cured with a small change in β.

4. ASTRONOMICAL CONSEQUENCES OF THE DEGRADED POLARIZATION

In this section we consider the impact on MMA astronomy of the polarization degradation estimated at the end of Section 3. Since the circularly polarized beams are separated on the sky the gain on the boresite axis of the antenna, that is the direction in which the two beams have equal gain, will be reduced. This gain loss will reduce sensitivity when observing small sources close to the antenna axis. The separated beams are shown in Figure 8 and Figure 9 shows the on-axis gain loss as a function of the amount of beam squint. The on axis gain loss for θ_s = .088 λ/D is only a little more than 1% so this is not a major effect. Note that with linearly polarized feeds the on-axis gain loss will be the same. Gain that is lost due to beam squint with circularly polarized feeds is lost due to reduced polarization efficiency with linearly polarized feeds. The co-polarized and cross-polarized patterns for the case of linear feeds are shown in Figure 10.

The major effect of the polarization degradation would be its effect on the ability of the MMA to measure polarization. Thompson (1976) provides a clear discussion of the issues for both circularly and linearly polarized feeds. Summarizing Thompson's conclusions for the VLA, linear polarization measurements should not be effected but circular polarization measurements are seriously compromised. In general these conclusions have been confirmed by experience at the VLA. Comparing the MMA circularly polarized beam separation of .14 beamwidths with the VLA separation of .06 beamwidths indicates

that the problem will be worse for the MMA than for the VLA. Figure 8 shows the instrumental circular polarization in the plane of the beamsquint and indicates values of about 25% and 40% respectively at the halfpower and tenthpower points in the primary beam. Holdaway et al (1992) and Vourlidas and Bastian (1993) discuss algorithms for removing the effect of the instrumental circular polarization.

The effect of these polarization problems on the ability of the MMA to do high dynamic range total intensity measurements needs to be investigated further. Thompson showed that the loss of circular symmetry of the primary beam should be acceptable for the VLA. It is not clear, however, that the approximations made by Thompson are reasonable with the larger beam squint of the MMA, especially when it is remembered that the MMA will frequently image the full primary beam or even, using mosaicing, multiple primary beams.

One final point should be kept in mind if an offset primary reflector is selected for the MMA. Even if the polarization problems at the secondary focus are solved using one of the methods discussed in Section 5, the poor performance at the primary focus will remain. This poor performance would include a 6 dB amplitude asymmetry across the aperture and a .18 beamwidth circularly polarized beam separation. There does not seem to be any strong reason why the prime focus should be needed in the future, but this would represent reduced flexibility to respond to currently unforeseen developments.

5. POSSIBLE SOLUTIONS TO THE POLARIZATION PROBLEMS

In this section we examine several possible ways of curing the secondary focus polarization problems.

5.1 Optimized Double Offset Geometry With Beam Waveguide Feed.

The basic problem with the MMA geometry is the large value of β needed to bring the optical path into the middle of the offset primary reflector where it is structurally desirable to locate the receiver cabin. A way of keeping β small and using the polarization correction properties of the optimized double offset geometry mentioned in Sections 1 and 2 is shown in Figure 11. In this geometry the secondary focus is located at F_1 with e = 1.11, $\beta = .16^\circ$ and $\theta_\beta = 3.0^\circ$. Then (3) gives $\alpha = 3.0^\circ$ and (4) gives $\theta_s = 0$. The secondary focus is transferred from F_1 to the desired position at F_2 using the two flat mirrors M1 and M2. There are several minor disadvantages with this geometry. There will probably be a few % loss of sensitivity associated with M1 and M2 especially in the longer wavelength bands. For a given focal ratio at the feed the subreflector has to be larger, making subreflector nutation more difficult. Keeping the optical path between the subreflector and M1 clear will complicate the design of the subreflector support arm. The blockage due to M2 is larger

than the hole needed to allow the beam to pass through the reflector surface. The beam could be brought to F2 underneath the reflector but this would complicate the task of keeping the beam free of obstructions. Finally, the finite size of M1 and M2 will probably limit the size of focal plane arrays for the longer wavelength bands. If further study does not identify more serious problems, this geometry does seem viable.

5.2 Polarization Correcting Tertiary reflector

The use of a tertiary reflector to correct the polarization of an Open Cassegrain was suggested by Chu and Turrin (1973) and the detailed theory of the technique is given by Dragone (1978). We will define the central ray in a dual reflector system as that ray from the secondary focus which, after reflection by the secondary and primary reflectors, passes through the center of the primary aperture. Suppose we use a tertiary reflector such as an ellipsoid to form a tertiary focus, as shown in Figure 12. Using symmetry arguments Dragone shows that this tertiary ellipsoid will correct the polarization if the parameters of the ellipsoid are chosen so that a ray travelling along the axis of the equivalent parabola through the secondary focus, after two reflections by the tertiary reflector, becomes the central ray. To achieve this the parameters of the tertiary must satisfy:

$$\tan(i) = \frac{M}{M-1}\tan(\gamma) \qquad (5)$$

where the angles i and γ are defined in Figure 12 and $M = -|F_2I|/|F_1I|$. There are many locations of F_2 with respect to F_1 and many ellipses which will satisfy (5). For convenience we will use the symmetric arrangement shown in Figure 13 in which the tertiary focus is arbitrarily placed on the line which bisects the angle between the axis of the equivalent parabola and the central ray. In this case it can be shown that the tertiary ellipsoid satisfying (5) has an eccentricity, e_t, given by:

$$e_t = \frac{1-\left|1-2\left(\cos\frac{\gamma}{2}\right)^2\right|}{\sin\gamma} \qquad (6)$$

We can now design a polarization correcting tertiary for the proposed MMA geometry shown in Figure 7. Note that $2\gamma = \pi-\alpha$. For the MMA geometry $\alpha = 17.5^\circ$. Then from (6) $e_t = 0.858$. Selecting the distance between the secondary and tertiary focus arbitrarily

to be 1m then gives the tertiary shown in Figure 14. There are a number of complications with the use of a tertiary in this way. The orientation of the feed shown in Figure 14 does not provide a suitable location for the receiver so it will be necessary to interpose a flat plate between the tertiary focus and the ellipsoid to direct the beam down into the receiver cabin. To make room for the tertiary and the flat plate above the receiver cabin it will be necessary to move the secondary focus up closer to the reflector surface and to use a slightly larger value for β. In the design shown in Figure 14 the top and bottom edges of the subreflector do not subtend equal angles at the feed. The parameters of the ellipsoid can be changed to cure this. With the tertiary so close to the feed it is likely at the longer wavelength bands that there will be undesirable diffraction effects and that the size of focal plane arrays will be limited. None of these complications seem so fundamental as to prevent the use of a polarization correcting tertiary.

5.3 Use of Shaped Reflectors

A shaped Open Gregorian geometry can be synthesized which has a symmetric aperture distribution (Galindo-Israel, 1991), so it is likely that a shaped design without polarization degradation is possible. This possibility has not been investigated at all because shaped reflector systems usually have severely limited fields-of-view and because a shaped offset primary probably would not be a surface of revolution, significantly increasing reflector panel cost. The shaped reflector approach should be investigated more to verify that these limitations are real.

5.4 Use of an Open Gregorian or Lower Magnification Geometry

With a Gregorian geometry the subreflector lies on the opposite side of the parent parabola axis, allowing the inside edge of the primary to be located right up against this axis without blockage. This leads to a slightly smaller value for β, thereby reducing the polarization degradation at both the primary and secondary foci slightly. The merits of a Gregorian geometry should therefore be investigated, but it is clear that the use of a Gregorian geometry alone cannot completely solve the problem. Evaluation of expressions (2), (3) and (4) as a function of eccentricity, for a given value of β, shows that the beam squint is essentially constant for all reasonable values of eccentricity for both Cassegrain ($e>1$) and Gregorian ($e<1$) geometries. Therefore the polarization degradation cannot be reduced by simply changing the focal ratio of the optics.

6. CONCLUSIONS

A MMA antenna using the Open Cassegrain geometry proposed by Cheng (1994) will have a separation between circularly polarized beams of 0.14 beamwidths (compared with .06 beamwidths on the VLA) or -22 dB cross polarized sidelobes in linear polarization. This will seriously limit the ability of the MMA to measure circular polarization. This degradation in polarization performance can be cured at the expense of a more complicated optics system using either of two approaches. An optimized double offset geometry can be used, with the secondary focus being transferred to the center of the primary using a pair of flat plate reflectors. Alternatively, a polarization correcting tertiary reflector can be used close to the secondary focus of the Open Cassegrain geometry. It must be noted that the analysis and synthesis of reflector geometries reported here is based purely on geometrical optics. Before any geometry is finally chosen for the MMA it is essential that a full diffraction analysis be performed to check that there are no unacceptable losses or limitations in the field-of-view for the longer wavelength bands.

ACKNOWLEDGMENTS

I thank J. Cheng, M. Holdaway, J. Payne and F. Owen for helpful discussions.

REFERENCES

Cheng, J., "Homologous Offset Antenna Concept For the Millimeter Array Project", MMA Memo 110, March 1994.

Chu, T-S. and Turrin, R.H., "Depolarization properties of offset reflector antennas," IEEE Trans. Antennas Propagat., vol AP-13, pp 339-345, 1973.

Cook, J.S., Elam, E.M. and Zucker, H.,"The Open Cassegrain Antenna: Part I. Electromagnetic Design and Analysis", BSTJ, vol 44, pp 1255-1300, 1965.

Dragone, C., "Offset Multireflector Antennas With Perfect Pattern Symmetry and Polarization Discrimination", BSTJ, vol 57, pp 2663-2684, 1978.

Duan, D-W. and Rahmat-Samii, Y., "Beam Squint Determination in Conic-Section Reflector Antennas with Circularly Polarized Feeds", IEEE Trans. Antennas and Propagat., vol AP-39, pp 612-619, 1991.

Gallindo-Israel, V., Imbriale, W.A., Mittra, R. and Shogen, K., "On the Theory of the Synthesis of Offset Dual-Shaped Reflectors - Case Examples", IEEE Trans. Antennas and Propag., vol AP-39, 620-626, 1991.

Holdaway, M.A., Carilli, C.L. and Owen, F., "Possible Algorithms to Improve the VLA's Polarization Performance", VLA Scientific Memo 163, 1992.

Rudge, A.W., Milne, K., Olver, A.D. and Knight, P., "The Handbook of Antenna Design", vol 1, Peter Peregrinus Ltd. pub., London, 1982.

Rusch, W.V., Prata, A., Rahmat-Samii, Y., Shore, R.A., "Derivation and Application of the Equivalent Paraboloid for Classical Offset Cassegrain and Gregorian Antennas", IEEE Trans. Antennas and Propagat., vol AP-38, pp 1141-1149, 1990.

Thompson, A.R., "The Effect of the Beam Offsets on Polarization Measurements", VLA Scientific Memo 125, July 1976.

Vourlidas, A. and Bastian, T., "Corrections of Beam Squint for the Improvement of Circular Polarization Measurements with the VLA", VLA Test Memo 180, 1993.

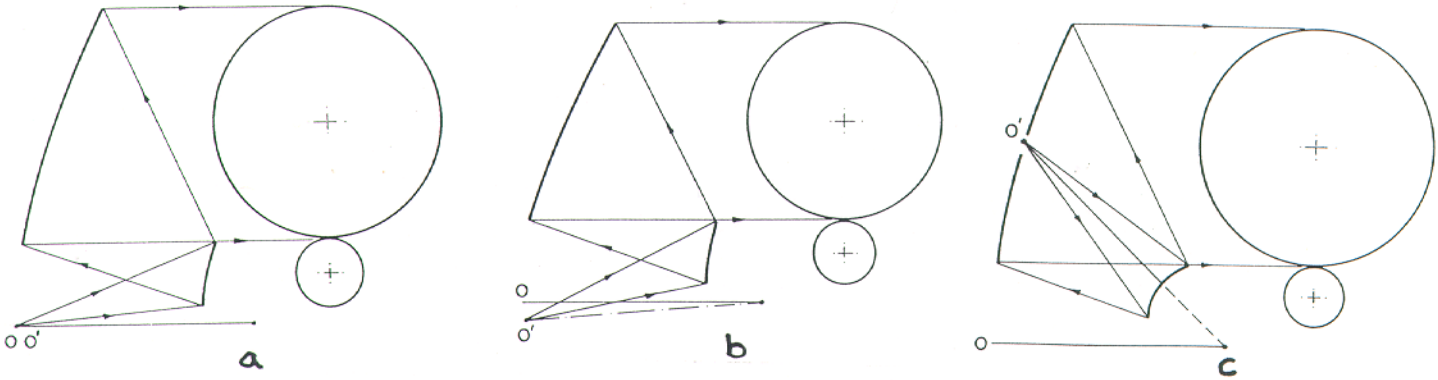

a Double-offset system;
b Optimised double offset;
c Open Cassegrainian system.
Paraboloid vertex at 0 and feed phase centre located at 0′

Figure 1. Dual-offset-reflector configurations (taken from Rudge et al, 1982).

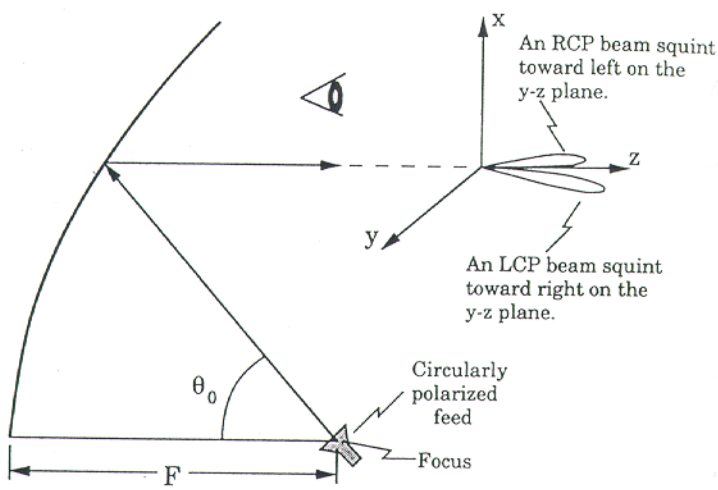

Figure 2. Prime focus fed parabola with tilted feed (taken from Duan and Rahmat-Samii, 1991).

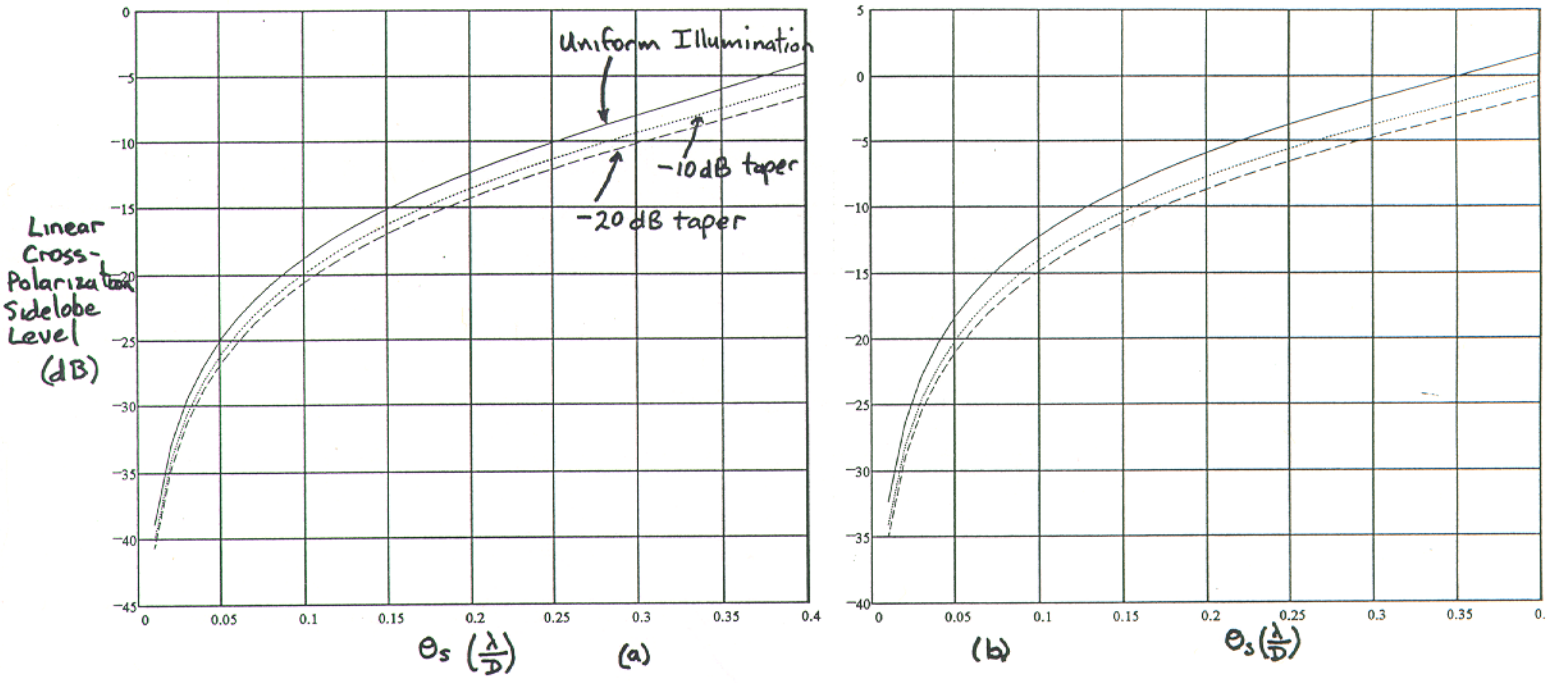

Figure 3. Amplitude of the cross polarized sidelobes for a linearly polarized feed as a function of the beam squint which would be present with a circularly polarized feed. (a) cross polarized level as a fraction of the peak of the main beam. (b) cross polarized level as a fraction of the main beam level at the same angle as the cross polarized peak.

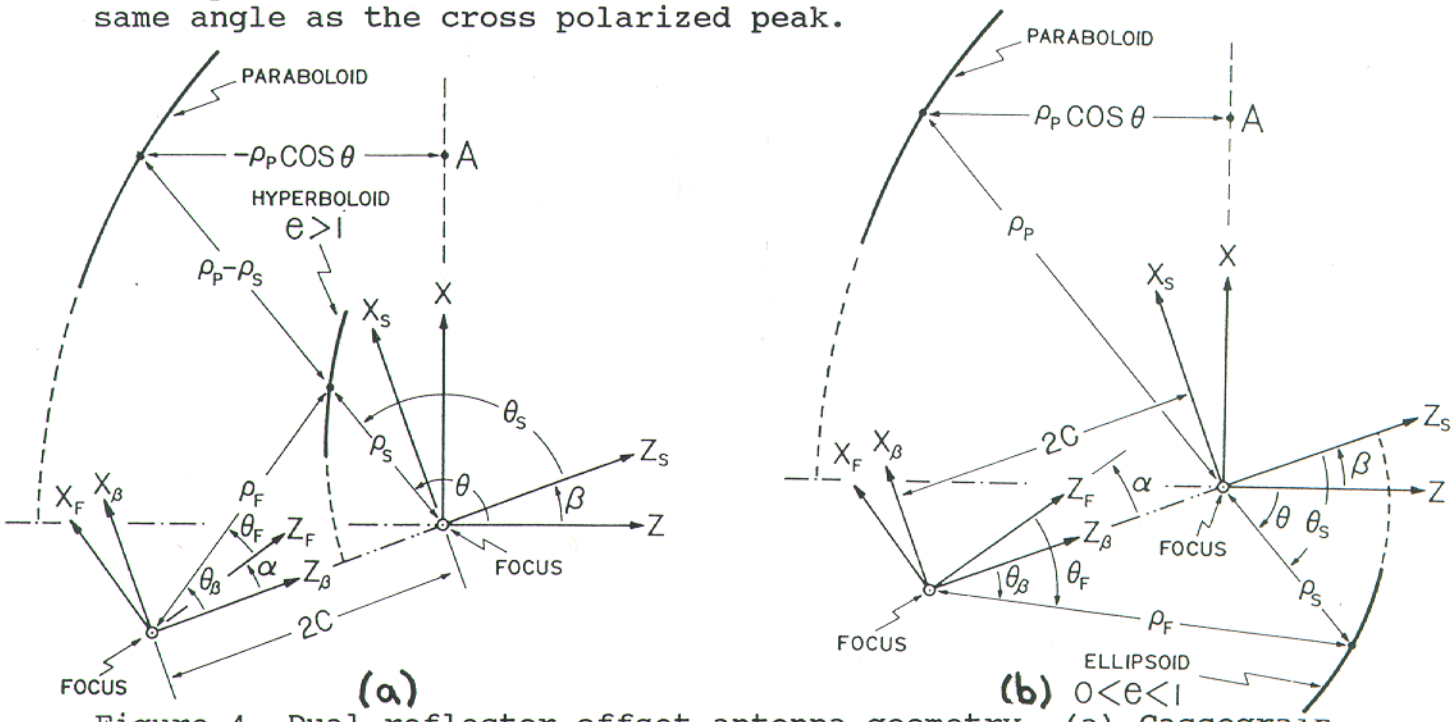

Figure 4. Dual reflector offset antenna geometry. (a) Cassegrain, (b) Gregorian, taken from Rusch et al, 1990.

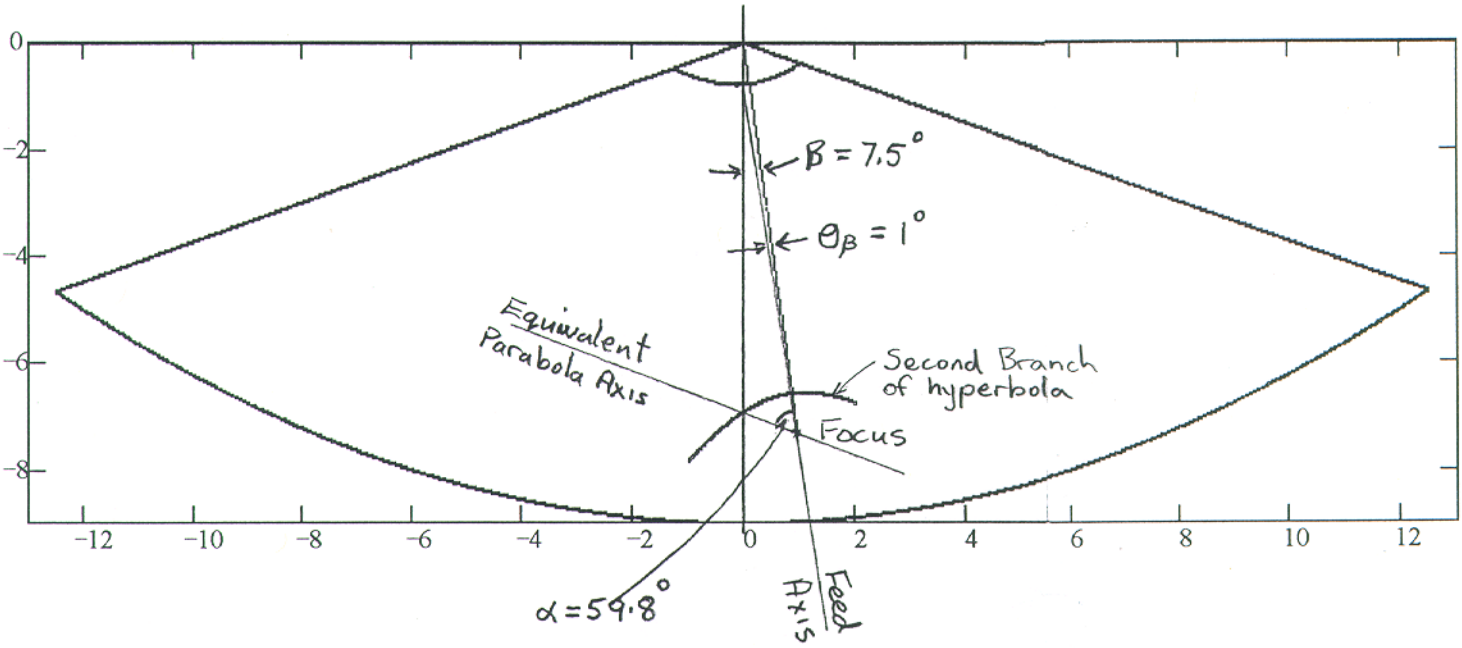

Figure 5. VLA classical Cassegrain geometry used to synthesize the shaped Cassegrain reflectors.

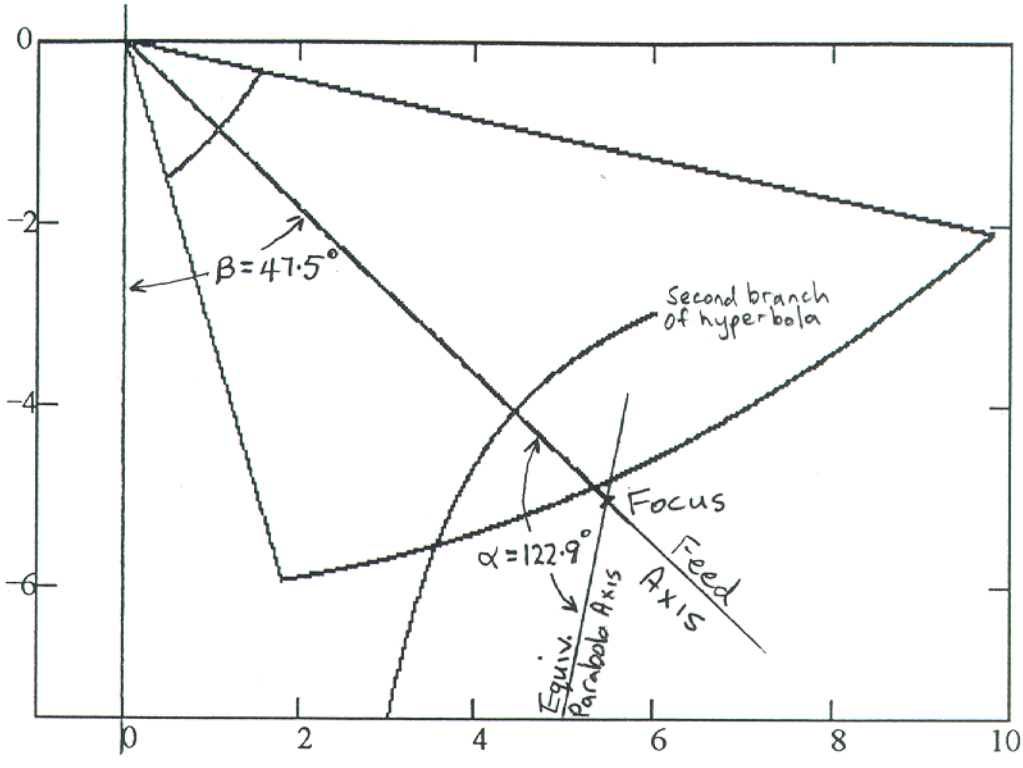

Figure 6. Geometry of Bell Labs Open Cassegrain antenna (Cook et al, 1965).

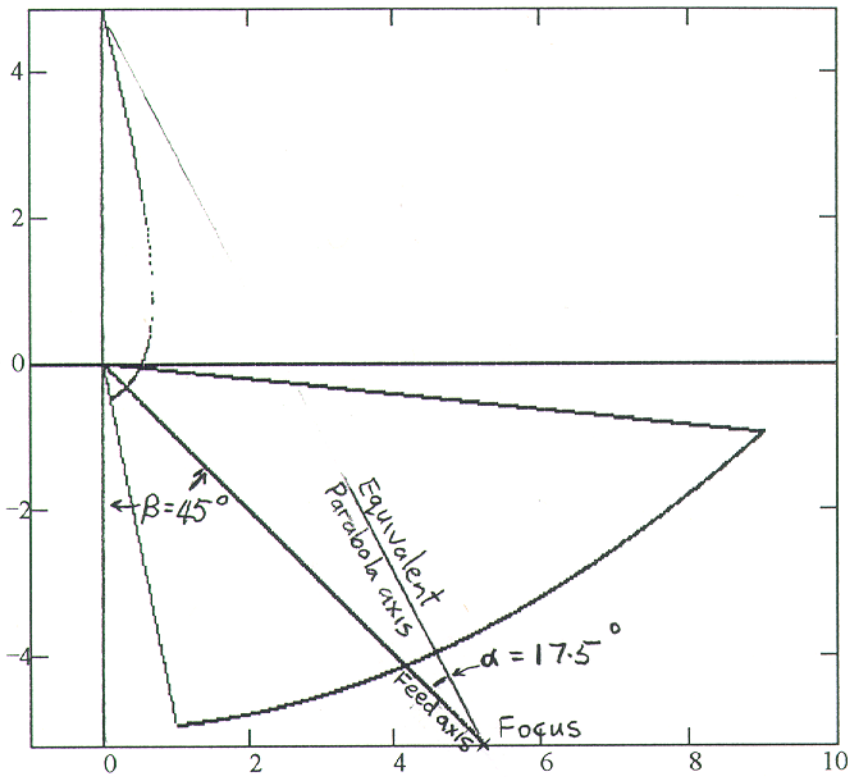

Figure 7. Geometry of proposed MMA design (Cheng, 1994).

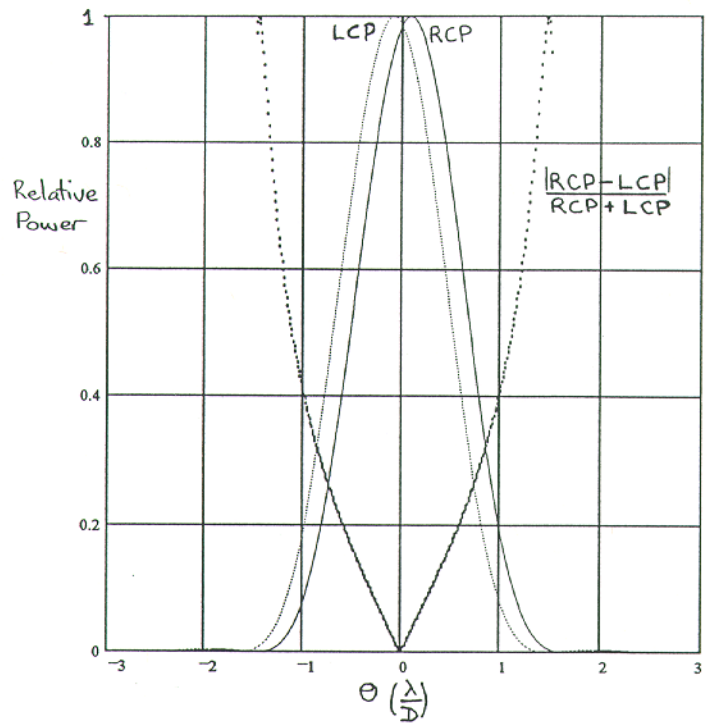

Figure 8. Separated beams for θ_s=.088 λ/D and a -10 dB aperture illumination taper. Also shown is the instrumental circular polarization given as the ratio of the difference to the sum of the two circularly polarized beams.

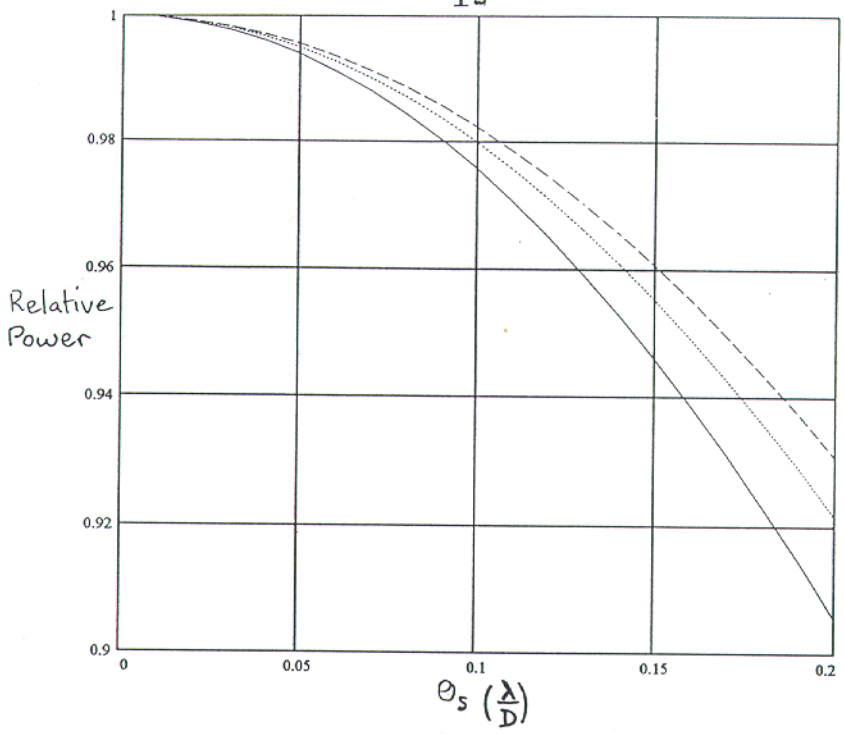

Figure 9. On axis gain loss as a function of beam squint.

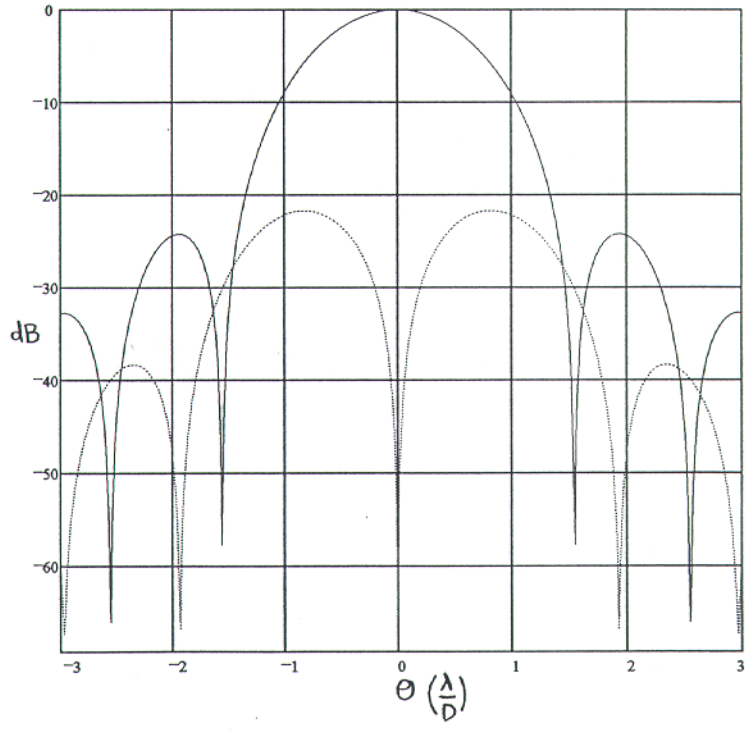

Figure 10. Main beam and cross polarized sidelobes for linearly polarized feed.

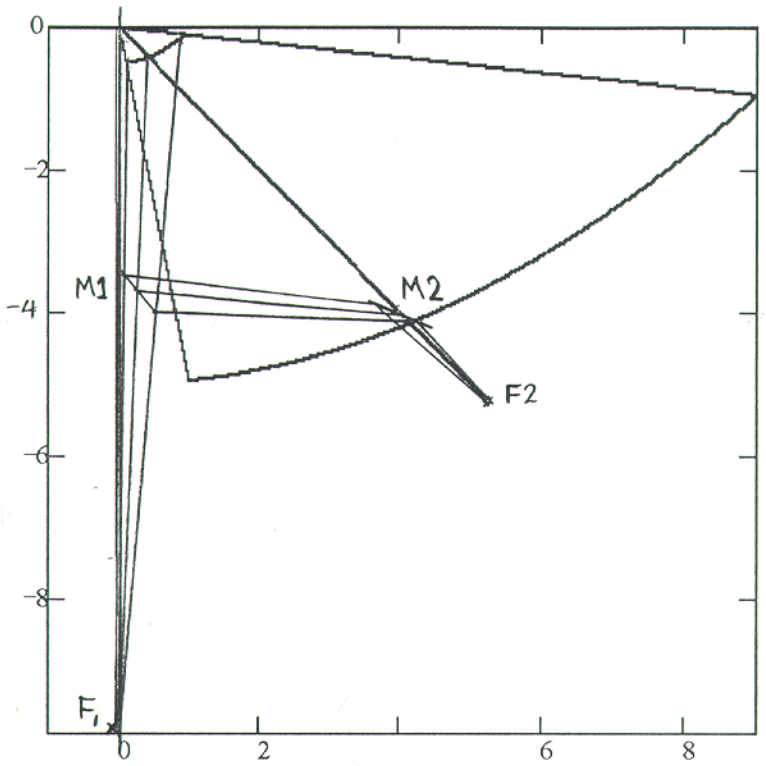

Figure 11. Optimised double offset geometry with flat plate beam waveguide feed.

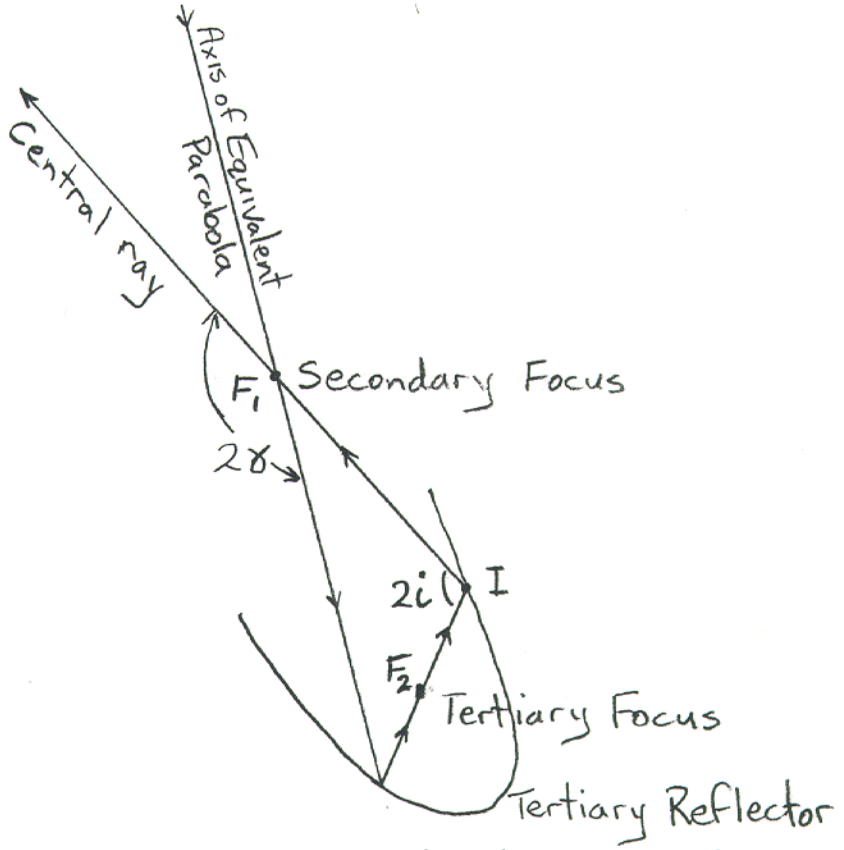

Figure 12. Tertiary reflector for polarization correction.

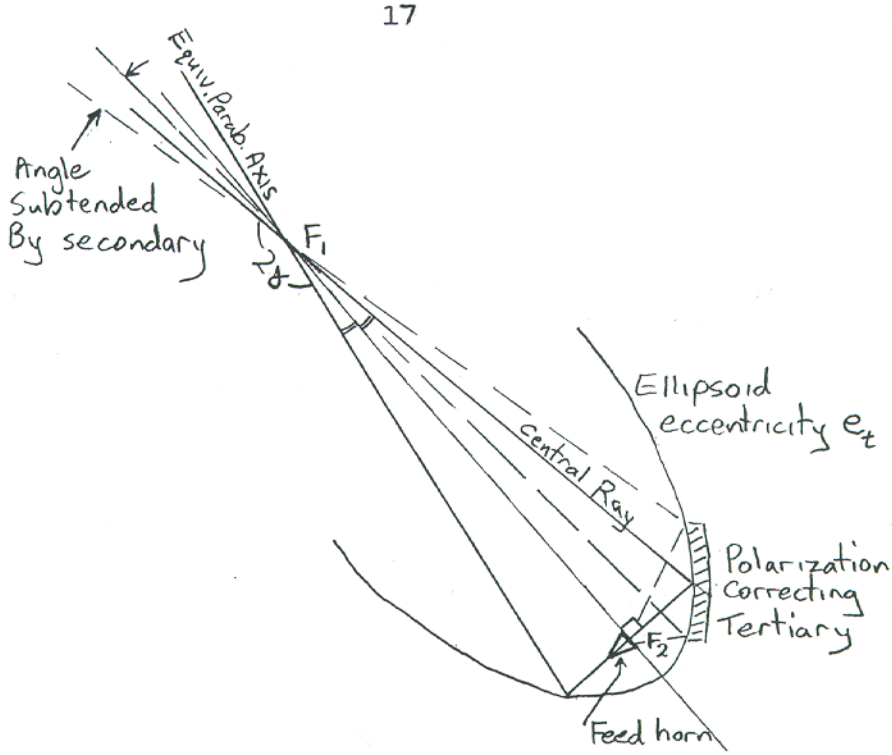

Figure 13. Tertiary reflector with tertiary focus on the bisector of the angle between the equivalent reflector axis and the central ray.

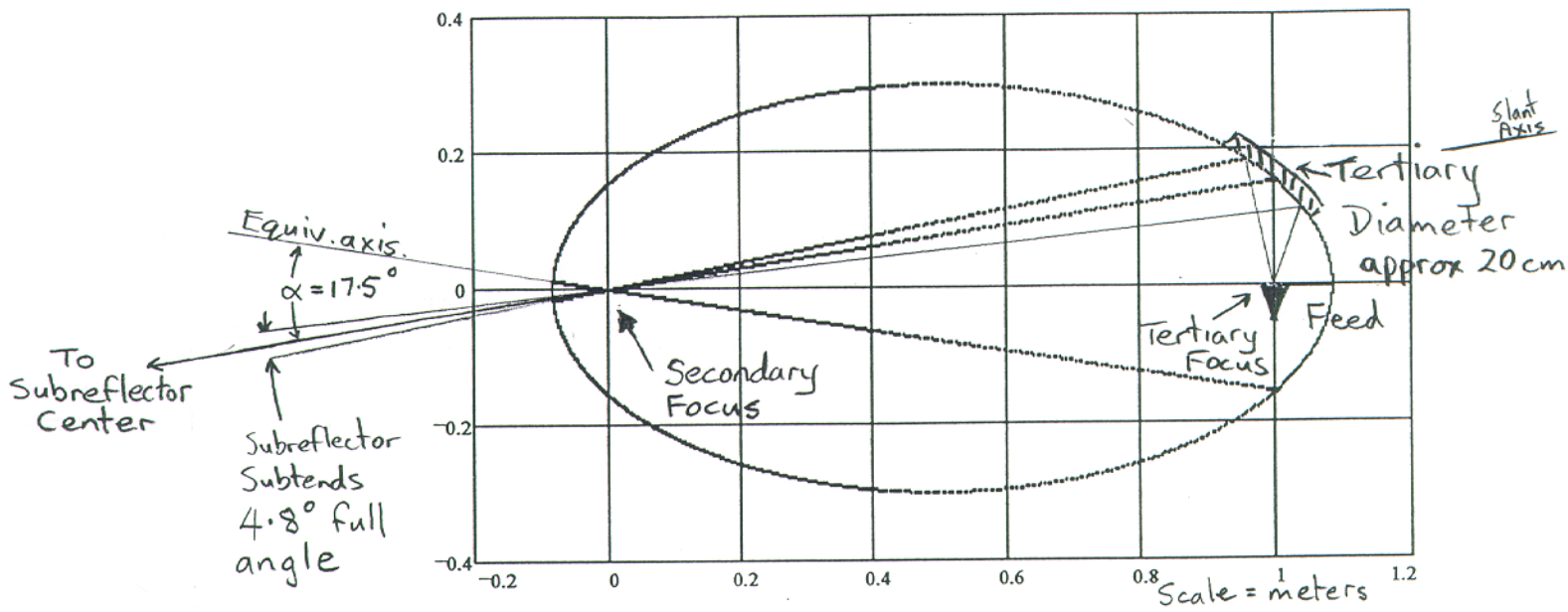

Figure 14. Tertiary reflector for proposed MMA Open Cassegrain.